

Analysis of Deep Learning-Based Colorization and Super-Resolution Techniques for Lidar Imagery

Sier Ha , Honghao Du , Xianjia Yu , Jian Song , Tomi Westerlund 

[†]Turku Intelligent Embedded and Robotic Systems (TIERS) Lab, University of Turku, Finland.
Emails: {sier.s.ha, honghao.h.du, jian.j.song, xianjia.yu, tovewe}@utu.fi

Abstract—Modern lidar systems can produce not only dense point clouds but also 360 degrees low-resolution images. This advancement facilitates the application of deep learning (DL) techniques initially developed for conventional RGB cameras and simplifies fusion of point cloud data and images without complex processes like lidar-camera calibration. Compared to RGB images from traditional cameras, lidar-generated images show greater robustness under low-light and harsh conditions, such as foggy weather. However, these images typically have lower resolution and often appear overly dark. While various studies have explored DL-based computer vision tasks such as object detection, segmentation, and keypoint detection on lidar imagery, other potentially valuable techniques remain underexplored. This paper provides a comprehensive review and qualitative analysis of DL-based colorization and super-resolution methods applied to lidar imagery. Additionally, we assess the computational performance of these approaches, offering insights into their suitability for downstream robotic and autonomous system applications like odometry and 3D reconstruction.

Index Terms—Lidar, Super-Resolution, Colorization, Lidar-as-a-camera

I. INTRODUCTION

Lidar and camera are extensively used as primary sensors for robotic and autonomous systems [1], [2]. While deep learning (DL) techniques have matured significantly for processing RGB images from cameras, their application to lidar point clouds remains limited due to the high computational complexity and the relatively sparse semantic content of point clouds beyond geometric structure. Recent advancements in lidars enable the generation of images alongside point clouds by encoding the reflectivity from either ambient light or emitted laser signals [3]. These lidar-generated images are more robust to motion blur, illumination changes, and adverse weather conditions such as fog. Furthermore, they simplify the fusion of images and lidar point clouds, reducing the complexity of online or offline lidar-camera fusion. However, these lidar-generated images are typically low resolution and appear dark challenging their further processing.

Nowadays, studies have begun exploring the adaptation of DL-based techniques that were originally designed for conventional RGB imagery to lidar-generated images, including applications in object detection, segmentation, and keypoint

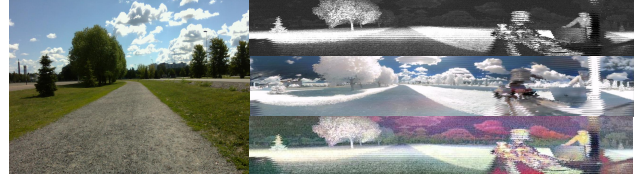


Fig. 1: DL-based super-resolution and colorization results for lidar image: RGB (left), lidar signal, colorized near-IR, and colorized signal images (right, top to bottom)

extraction [4], [5]. Nevertheless, this area remains underexplored, and other potentially valuable DL approaches, such as super-resolution and colorization, have not been thoroughly evaluated. Super-resolution could enhance the spatial detail of panoramic lidar images, while colorization may enrich pixel-level information, offering potential benefits for tasks such as odometry and 3D reconstruction. Fig. 1 illustrates our evaluation of one of the DL-based super-resolution and colorization approaches applied to lidar images. The image on the left is an RGB image, while the images on the right (top to bottom) include one type of raw lidar image and its enhanced version via DL based super resolution and colorization.

To address these gaps, we present a comprehensive review of state-of-the-art DL-based super-resolution and colorization methods, surpassing the scope of prior surveys (Section II). Building on this foundation, we qualitatively evaluate several representative approaches on lidar-generated images from both indoor and outdoor datasets (Section III). We report the runtime performance of each method, providing insights for their potential deployment in real-world robotic systems.

II. DL BASED SUPER-RESOLUTION AND COLORIZATION

A. DL-based Colorization

DL-based colorization is commonly used in image restoration and thermal infrared image colorization. Table I shows the existing approaches we have reviewed with the consideration of applied environments, implementation availability, programming language compatibility, and a brief description.

DeOldify [6] is a DL-based tool that is used to colorize and restore old black and white images and videos using

TABLE I: Brief Comparison of Deep Learning-based Colorization Models

Model	Indoor	Outdoor	Code	Description	Language compatible
<i>DeOldify</i> [6]	✓	✓	✓	Effectiveness in restoring and colorizing old black-and-white photos	Python3
<i>DDColor</i> [7]	✓	✓	✓	Utilizes diffusion models for high-quality image colorization	Python3
<i>BigColor</i> [8]	✓	✓	✓	Designed for large-scale, high-resolution image colorization	Python3
<i>BigGAN</i> [9]		✓		Generating high-resolution, high-fidelity natural images	
<i>PearlGAN</i> [10]		✓	✓	Focuses on colorizing thermal and infrared images using GANs, effective in outdoor environments	Python3
<i>I2V-GAN</i> [11]		✓	✓	GAN-based model for colorizing infrared to visible spectrum images	Python3
<i>Colorful Image Colorization</i> [12]	✓	✓	✓	One of the first CNN-based colorization models, introducing probabilistic color assignment	Python3
<i>Let there be Color</i> [13]	✓	✓	✓	A fully automatic image colorization method that works on both grayscale and natural images using deep learning	Lua
<i>DISCO</i> [14]	✓	✓	✓	Uses deep neural networks to provide automatic colorization with a focus on preserving detail and texture	Python3
<i>Deep Koalarization</i> [15]	✓	✓	✓	Combines a pre-trained VGG network with a colorization model for realistic colorization	Python3
<i>Palette</i> [16]	✓	✓	✓	A versatile colorization model that leverages palette-based techniques to achieve high-quality results across various image types	Python3
<i>ChromaGAN</i> [17]	✓	✓	✓	GAN-based model that emphasizes perceptual loss for natural colorization results	Python3
<i>InstColorization</i> [18]	✓	✓	✓	An instance-aware colorization model that handles complex scenes by focusing on individual object instance	Python3
<i>SCGAN</i> [19]	✓	✓	✓	A self-consistent GAN-based colorization approach that ensures color consistency across different regions of an image	Python3

the NoGAN techniques. The generator network learns to add colour to the greyscale image, while the discriminator network learns to differentiate between the real colour image and the generator-generated image. Compared to the traditional GAN model, this model prioritizes natural colors and performs well and consistently on landscapes.

The core concept of the DDColor [7] model is the use of two distinct decoders for image colorization. The Pixel Decoder focuses on recovering spatial details and image structure, while the Colour Decoder learns semantically aware color representations from visual features at multiple scales. By combining the outputs of both decoders, DDColor aims to produce more natural and vivid colors, especially in complex scenes with multiple objects.

BigColor [8] serves as a precursor to the DDColor model, which builds upon and refines the foundations established by BigColor. This model introduces a novel approach based on BigGAN [20], expanding the representation space and offering a range of coloring results.

BigGAN is a colorization model for generating high-resolution, high-fidelity natural images based on Large Scale GAN Training for High Fidelity Natural Image Synthesis [21] training. The framework consists of a generator and a discriminator. The generator creates images, the discriminator evaluates them against real images, and then iteratively trains to generate high quality images.

PearlGAN [10] is tailored for converting nighttime thermal infrared (NTIR) images into daytime color (DC) images. It excels at producing high-quality colorization for NTIR images of open roads. PearlGAN is restricted to outdoor scenes, and its colorization capabilities are primarily focused on roads and trees, particularly in lidar-generated images.

I2V-GAN [11] is designed for unpaired infrared-to-visible video translation. Like PearlGAN, it is specialized for outdoor scenes and works with infrared images. I2V-GAN facilitates the conversion of infrared video data into visible spectrum equivalents, although it shares similar limitations in its applicability to specific scene types and environments.

Let There Be Color [13] is a Convolutional Neural Network (CNN) trained using paired grayscale and color images. The model learns to colorize grayscale images by leveraging the correlations between the grayscale inputs and their correspond-

ing color images. It employs a deep architecture to capture complex patterns and color distributions, resulting in visually appealing colorization of grayscale images. The approach effectively handles a variety of image types, providing robust colorization across different scenes.

DISCO [14] provides a new method of colouring images by separating colour representation from spatial information, helping to produce images with vibrant and realistic colors.

Deep Koalarization [15] combines CNNs with the advanced Inception-ResNet-v2 architecture, allowing it to capture complex details and nuances in images. The model leverages Inception modules for efficiently handling multi-scale features, while ResNet’s residual connections enable deeper networks to be trained without encountering gradient vanishing issues. The model’s complexity and high computational demands require significant processing power and memory. Paltte [16] is similar to Deep Koalarization, as it reproduces the full model.

ChromaGAN [17] by utilizing an adversarial framework, ChromaGAN’s network of generators and discriminators work in tandem to produce high-quality color images. Where the generator network learns to generate color images from grayscale inputs, the discriminator network evaluates the veracity of these colorizations. Like many GAN-based models, ChromaGAN requires significant computational resources and is a complex and time-consuming process.

Instance-aware Image Colorization [18] Enhance coloring accuracy and fidelity by incorporating instance-level perception into the process. The model distinguishes between different instances of the same object class in an image, enabling more accurate and consistent application of color. The complexity of the model and instance-level segmentation increases the computing time.

SCGAN [19] is the use of saliency maps to inform the generator network within the GAN framework to ensure that the generated colors are visually appropriate, which is particularly beneficial for images with complex compositions or where certain objects should stand out.

B. DL-based Super Resolution

DL has greatly advanced the development of image super-resolution, enabling the models to generate high-quality magnified images from low-resolution inputs. This part provides a comparative analysis of various DL super-resolution models,

TABLE II: Brief Comparison of Deep Learning based Super Resolution Models

Model	Code	Architecture	Training Data	Strengths	Weaknesses	Language compatible
<i>SRCNN</i> [22]		3-layer CNN	ImageNet	Simple, Effective	Limited long-range dependency capture	
<i>VDSR</i> [23]		20-layer CNN	ImageNet	Deep architecture, Residual learning	High computational cost	
<i>SRGAN</i> [24]		CNN with GAN	ImageNet, DIV2K	High perceptual quality	Potential artifacts	
<i>DRRN</i> [25]		Recursive Residual Network	ImageNet, DIV2K	Parameter efficient, Deep architecture	High computational cost	
<i>CARN</i> [26]	✓	Cascading Residual Network	DIV2K	Lightweight, Fast inference	Slightly lower accuracy	Python3
<i>SwinIR</i> [27]	✓	Transformer-based	DIV2K, Flickr2K	High performance, Handles large scale factors	High computational cost	Python3
<i>SCUNet</i> [28]	✓	CNN with Spatially Consistent Normalization	DIV2K	Maintains spatial consistency, Effective edge preservation	High computational resources, Training complexity	Python3
<i>ESRGAN</i> [29]	✓	GAN with Residual-in-Residual Dense Blocks	DIV2K, Flickr2K	Realistic textures, Superior perceptual quality	High computational cost, Can produce artifacts	Python3
<i>DCSCN</i> [30]	✓	CNN and Sparse Coding	CIFAR-10, ImageNet	Efficient high frequency detail capture	Struggles with complex images	Python3
<i>CAT</i> [31]	✓	Cross-Attention Transformer	DIV2K, Flickr2K	Strong cross-modal learning, High fidelity	Computationally expensive	Python3
<i>Perceptual Losses</i> [32]		CNN with Perceptual Loss	MS-COCO, ImageNet	High-quality image generation, Real-time performance	Dependent on pre-trained networks, Generalization limits	
<i>SinGAN</i> [33]	✓	GAN with Single Image Learning	Single Image	Effective for artistic enhancement, Versatile	Training on each image required, Limited scalability	Python3
<i>DnCNN</i> [34]	✓	Deep CNN with Batch Normalization	ImageNet, BSD400	Effective denoising, Simple architecture	Limited to small scale factors	Python3
<i>SR3</i> [35]	✓	Diffusion Model for SR	CelebA-HQ, FFHQ	Generates realistic and high-quality images	High computational cost, Slow inference	Python3

describing their architecture, performance, programming language compatibility, advantages, and disadvantages (Table II).

SRCNN [22] is one of the pioneering DL models for image super-resolution. Its three-layer CNN is designed for feature extraction, non-linear mapping, and reconstruction. Trained on ImageNet with mean square error (MSE) as the loss function, SRCNN aims to minimize the difference between the output and the ground truth image. It achieves strong results on datasets like Set5, Set14, and BSD. Owing to its shallow architecture, SRCNN struggles to capture long-range dependencies in complex images, limiting its overall performance.

VDSR [23] model builds on the SRCNN framework by employing a much deeper CNN with 20 layers. This increased depth enables VDSR to learn more complex mappings from low- to high-resolution images, significantly improving performance. To mitigate the vanishing gradient problem, the model incorporates residual learning. VDSR consistently outperforms SRCNN on benchmark datasets, showcasing the benefits of its deeper architecture for super-resolution tasks. However, the added depth results in higher computational costs.

SRGAN [24] was the first to apply generative adversarial networks (GANs) to super-resolution tasks. SRGAN comprises two neural networks: a generator that creates realistic high-resolution (HR) images from low-resolution (LR) inputs, and a discriminator that distinguishes between generated images and real HR photos. Nevertheless, the adversarial training can introduce artifacts, and achieving a balance between the generator and discriminator remains challenging.

DRRN [25] leverages deep recursive learning with recursive residual blocks to effectively capture dependencies across different scales. DRRN employs a recursive structure with shared parameters, allowing it to increase network depth without significantly inflating the number of parameters. The recursive design complicates the training process and can be computationally intensive.

CARN [26] is a ResNet-based image super-resolution model designed for real-time applications. By using cascading connections, CARN reduces computational cost while retaining high performance, enabling it to merge features across layers and capture intricate image details more effectively. Trained on large-scale super-resolution datasets, CARN strikes a balance

between speed and accuracy, though its efficiency-focused design can lead to slight compromises in image quality compared to more complex models.

SwinIR [27] leverages the Swin Transformer architecture for tasks like super-resolution. By dividing images into smaller patches and analyzing them at multiple scales, SwinIR captures both local details and long-range dependencies. This method enhances the model’s understanding of the image’s global structure, although it increases computational complexity.

SCUNet [28] proposes a method to enhance image quality by removing noise without prior knowledge of its properties. This is done by integrating SCUNet with a strategic data synthesis process. It outperforms traditional and state-of-the-art models in denoising tasks, effectively eliminating noise while preserving details and textures. However, its high computational demands and reliance on synthetic data are key concerns for practical deployment.

ESRGAN [29] improves upon the ESRGAN model by introducing Residual Dense Blocks (RRDB) and Perceptual Loss Functions to enhance image realism. ESRGAN trains generators and discriminators simultaneously, resulting in superior image quality. ESRGAN is computationally demanding, requiring substantial processing power, memory, and numerous iterations for optimal results. Additionally, ESRGAN can produce artifacts, particularly in images with complex textures.

DCSCN [30] leverages deep CNNs, skip connections, and Network-in-Network (NIN) architectures to improve super-resolution image quality while maintaining computational efficiency. This enables the generation of high-quality images with fine details and textures. Despite its efficient design, the deep architecture and NIN layers still require considerable processing power and memory. Moreover, if not properly normalized, the model’s strong feature extraction may cause overfitting, affecting performance on unseen data.

CAT [31] uses a cross-attention mechanism to aggregate features from different image regions, enabling recovery of fine details and textures often lost in traditional methods. It also allows the model to efficiently handle various restoration tasks, including denoising, deblurring, and super-resolution. However, the complexity and computational demands of transformer architectures remain challenging and require substan-

tial processing power.

Perceptual Losses [32] utilizes a perceptual loss function to enhance the visual quality of generated images, using high-level feature differences from a pre-trained CNN, rather than relying on traditional pixel-by-pixel comparisons. Despite its advantages, the model’s reliance on pre-trained networks for perceptual loss calculations may limit its adaptability across different datasets, as performance may depend on the characteristics of the specific network used.

SinGAN [33] generates images by training a generative adversarial network (GAN) on a single image, allowing it to produce diverse outputs that preserve the original image’s texture, color, and structure. While its single-image capability is an advantage, SinGAN is computationally intensive, and its results can lack diversity compared to models trained on large datasets. Moreover, the quality of generated images depends heavily on the original image’s characteristics.

DnCNN [36] employs a deep CNN combined with NIN architecture and skip connections. These connections help integrate NIN layers, enhancing DnCNN’s ability to capture fine details and represent high-frequency components, improving texture and edge preservation in super-resolution images. However, without adequate regularization, DnCNN’s strong feature extraction capabilities can lead to overfitting, potentially affecting performance on unseen data.

SR3 [35] enhances image resolution in multiple stages, with each iteration refining the output of the previous one. This progressively improves quality, producing finer details and more accurate textures in the final high-resolution image. However, the iterative process increases computational demands, which may limit its use in real-time applications or resource-constrained environments.

The comparison of these models include evolution from simple CNNs to complex transformer-based architectures. The summary in Table II provides a clear visual comparison.

III. EVALUATION ON LIDAR IMAGERY

a) Dataset for Evaluation: We conduct all evaluations using open-source multi-modal LiDAR datasets [2], [37], focusing on data from the Ouster LiDAR. Its specifications are listed in Table III. Ouster provides dense point clouds and multiple image types: range, signal, and ambient images, encoding depth, IR intensity, and ambient light, respectively. We primarily use signal images, which have shown strong performance in prior work [5].

TABLE III: Specifications of Ouster OS0-128.

	IMU	Type	Channels	Image Resolution
Ouster OS0-64	ICM-20948	spinning	128	1024 × 128
FoV	Angular Resolution	Range	Freq	Points
360° × 90°	V : 0.7°, H : 0.18°	50 m	10 Hz	2,621,440 pts/s

The evaluation data sequences include indoor and outdoor environments. The outdoor environment is from the normal

road and a forest, denoted as *Open road* and *Forest*, respectively. The indoor data includes a hall in a building and two rooms, denoted as *Hall (large)*, *Lab space (hard)*, and *Lab space (easy)*, respectively. Our own *Forest* dataset was collected within a forested area.

b) Analysis of Colorization Approaches: Section II-A presented a comprehensive survey on the DL-based colorization approaches. Here, we qualitatively analyze the performance of the approaches on lidar-generated images (signal images), utilizing publicly available code repositories on GitHub. The evaluation methods were selected based on their implementation availability and ease of deployment on a standard laptop. More specifically, the approaches examined include *BigColor*, *Colorful Image Colorization*, *DDColor*, *De-Oldify*, *DISCO*, *InstColorization*, *Let there be color*, *PearlGAN*, as detailed in Table I.

c) Analysis of Super-Resolution Approaches: The review of the DL-based super-resolution approaches is in Section II-B. Among these approaches, we select the methods based on the same principle mentioned above: the availability of implementation and the simplicity of deployment for a standard laptop. The approaches included in the part are *CARN*, *SwinIR*, *DCSCN*, *ESRGAN*, *SCUNET*, as detailed in Table II. We qualitatively evaluate the super-resolution performance of these approaches on signal images.

d) Hardware Information: The evaluation was conducted using a Razer Blade 15 laptop by Ubuntu 22.04.4 LTS equipped with an Intel Core i7-12800H-20 processor, 16 GB of RAM with a frequency of 4800 MHz, and a GeForce RTX 3070 Ti GPU with 8 GB of memory.

IV. EXPERIMENTAL RESULTS

This section presents the qualitative evaluation results of DL-based super-resolution and colorization models. Following this analysis, the most suitable models in terms of both processing speed and output quality based on our experimental findings are selected. These models are then applied to our point cloud sampling approach for further performance analysis in terms of accuracy and the number of points extracted.

a) Super-Resolution of lidar imagery: The example processed images in Fig. 3a-3d, like most super-resolution models, the final rendering for the signal image has a higher degree of sharpening or an overall smoother image than the raw image in Fig. 2. Table V shows the inference speeds of the multiple popular DL-based super-resolution models with input and output sizes illustrated. The DL-model *CARN* demonstrates relatively high result quality, as illustrated in Fig. 3a and 3b, while also exhibiting fast processing speed.

b) Colorization of LiDAR imagery: Fig. 3e and 3f as well as Fig. 3g and 3h show the result of the two colorization models after coloring, which present different results due to the differences in the training datasets. Table V shows the inference speed of the multiple popular DL-based colorization models with input and output sizes illustrated. The DL model

TABLE IV: Comparison of running speed of each super-resolution model based on local environment

Model	Input size	Output size	Running speed (secs/image)
CARN	(1024, 128)	(2048, 256)	0.005
SwinIR	(1024, 128)	(4096, 512)	2.217
DCSCN	(1024, 128)	(2048, 256)	0.238
ESRGAN	(1024, 128)	(4096, 512)	2.667
SCUNET	(1024, 128)	(1024, 128)	1.706

DeOldify produces good colorization results, as shown in Fig. 1 and Fig. 3e and 3f, while demonstrating relatively faster processing speed, as indicated in Table V.

TABLE V: Comparison of running speed of each colorization model based on local environment

Model	Input size	Output size	Running speed (secs/image)
BigColor	(1024, 128)	(1024, 128)	0.54
Colorful Image Colorization	(1024, 128)	(1024, 128)	0.27
DDColor	(1024, 128)	(1024, 128)	0.37
DeOldify	(1024, 128)	(1024, 128)	0.23
DISCO	(1024, 128)	(1024, 128)	3.27
InstColorization	(1024, 128)	(256, 256)	0.05
PearlGAN	(1024, 128)	(1024, 128)	0.28

V. CONCLUSION AND FUTURE WORK

This paper provided a more comprehensive review of existing DL-based super-resolution and colorization methods than other literature. In this work, we have demonstrated the effectiveness of the DL-based super-resolution and colorization on lidar imagery. Additionally, we provide a runtime speed evaluation of those popular approaches on lidar imagery, posing the further application of these approaches in robotic and autonomous systems. Further research could focus on leveraging these methods to enhance lidar odometry or 3D reconstruction performance. Additionally, our experiments demonstrated that applying super-resolution and colorization techniques effectively reduced false detections made by the YOLOv11 instance segmentation model¹, as illustrated in Figure 4. For instance, the original NIR image in Figure 4a (top-left) incorrectly identifies a building as a bus (top-right); however, this misclassification is successfully avoided in the enhanced image (bottom-right). A similar improvement is also evident in the lidar reflectivity image shown in Figure 4b. Although a systematic analysis was not conducted, these preliminary observations hold potential value for researchers working in related fields.

ACKNOWLEDGMENT

This research is supported by the Research Council of Finland’s Digital Waters (DIWA) flagship (Grant No. 359247) and the DIWA Doctoral Training Pilot project funded by the Ministry of Education and Culture (Finland).

¹github.com/ultralytics/ultralytics

REFERENCES

- [1] S. Jiang, S. Wang, Z. Yi, M. Zhang, and X. Lv. Autonomous navigation system of greenhouse mobile robot based on 3d lidar and 2d lidar slam. *Frontiers in plant science*, 13, 2022.
- [2] H. Sier, Q. Li, X. Yu, J. Peña Queraltá, Z. Zou, and T. Westerlund. A benchmark for multi-modal lidar slam with ground truth in gnss-denied environments. *Remote Sensing*, 15(13), 2023.
- [3] A. Pacala. Lidar as a camera – digital lidar’s implications for computer vision. *Ouster Blog*, 2018.
- [4] X. Yu, S. Salimpour, J. P. Queraltá, and T. Westerlund. General-purpose deep learning detection and segmentation models for images from a lidar-based camera sensor. *Sensors*, 23(6), 2023.
- [5] H. Zhang, X. Yu, S. Ha, and T. Westerlund. Lidar-generated images derived keypoints assisted point cloud registration scheme in odometry estimation. *Remote Sensing*, 15(20), 2023.
- [6] J. Antic. Deoldify—a deep learning based project for colorizing and restoring old images (and video!), 2019.
- [7] X. Kang, T. Yang, W. Ouyang, P. Ren, L. Li, and X. Xie. Ddcolor: Towards photo-realistic image colorization via dual decoders. In *Proc. of the IEEE/CVF Int. Conf. on Computer Vision*, 2023.
- [8] G. Kim, K. Kang, S. Kim, H. Lee, S. Kim, J. Kim, S.-H. Baek, and S. Cho. Bigcolor: Colorization using a generative color prior for natural images. In *European Conf. on Computer Vision*. Springer, 2022.
- [9] A. Brock, J. Donahue, and K. Simonyan. Large scale GAN training for high fidelity natural image synthesis. In *Int. Conf. on Learning Representations*, 2019.
- [10] F. Luo, Y. Li, G. Zeng, P. Peng, G. Wang, and Y. Li. Thermal infrared image colorization for nighttime driving scenes with top-down guided attention. *IEEE Transactions on Intelligent Transportation Systems*, 2022.
- [11] S. Li, B. Han, Z. Yu, C. H. Liu, K. Chen, and S. Wang. I2v-gan: Unpaired infrared-to-visible video translation. In *ACMMM*, 2021.
- [12] R. Zhang, P. Isola, and A. A. Efros. Colorful image colorization. In *ECCV*, 2016.
- [13] S. Iizuka, E. Simo-Serra, and H. Ishikawa. Let there be Color!: Joint End-to-end Learning of Global and Local Image Priors for Automatic Image Colorization with Simultaneous Classification. *ACM Transactions on Graphics (Proc. of SIGGRAPH 2016)*, 35(4), 2016.
- [14] M. Xia, W. Hu, T.-T. Wong, and J. Wang. Disentangled image colorization via global anchors. *ACM Transactions on Graphics (TOG)*, 41(6):204:1–204:13, 2022.
- [15] F. Baldassarre, D. G. Morín, and L. Rodés-Guirao. Deep koalarization: Image colorization using cnns and inception-resnet-v2. *CoRR*, abs/1712.03400, 2017.
- [16] E. Wallner. Coloring-greyscale-images.
- [17] P. Vitoria, L. Raad, and C. Ballester. Chromagan: Adversarial picture colorization with semantic class distribution. In *The IEEE Winter Conf. on Applications of Computer Vision*, 2020.
- [18] J.-W. Su, H.-K. Chu, and J.-B. Huang. Instance-aware image colorization. In *IEEE Conf. on Computer Vision and Pattern Recognition (CVPR)*, 2020.
- [19] Y. Zhao, L.-M. Po, K.-W. Cheung, W.-Y. Yu, and Y. Abbas Ur Rehman. Scgan: Saliency map-guided colorization with generative adversarial network. *IEEE Transactions on Circuits and Systems for Video Technology*, 31(8), 2020.
- [20] A. Brock, J. Donahue, and K. Simonyan. Large scale gan training for high fidelity natural image synthesis, 2019.
- [21] A. Brock, J. Donahue, and K. Simonyan. Large scale gan training for high fidelity natural image synthesis, 2019.
- [22] C. Dong, C. C. Loy, K. He, and X. Tang. Image super-resolution using deep convolutional networks. *IEEE transactions on pattern analysis and machine intelligence*, 38(2), 2015.
- [23] J. Kim, J. K. Lee, and K. M. Lee. Accurate image super-resolution using very deep convolutional networks. In *Proc. of the IEEE Conf. on computer vision and pattern recognition*, 2016.
- [24] C. Ledig, L. Theis, F. Huszár, J. Caballero, A. Cunningham, A. Acosta, A. Aitken, A. Tejani, J. Totz, Z. Wang, et al. Photo-realistic single image super-resolution using a generative adversarial network. In *Proc. of the IEEE Conf. on computer vision and pattern recognition*, 2017.



(a) Raw image indoor



(b) Raw image outdoor

Fig. 2: Raw images of indoor and outdoor environment



(a) Example of CARN super-resolution indoor image



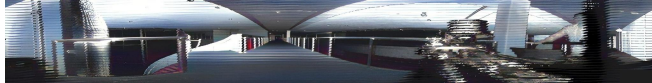
(b) Example of CARN super-resolution outdoor image



(c) Example of SCUNET super-resolution indoor image



(d) Example of SCUNET super-resolution outdoor image



(e) Example of DeOldify colorization indoor image



(f) Example of DeOldify colorization outdoor image

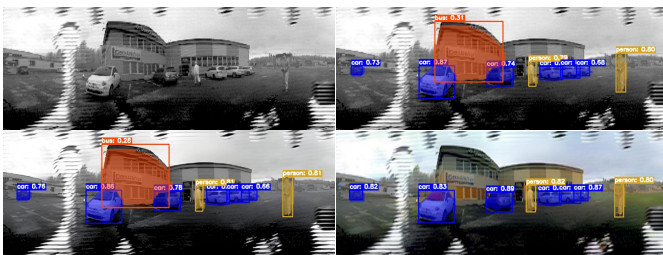


(g) Example of DDColor colorization indoor image



(h) Example of DDColor colorization outdoor image

Fig. 3: Examples of using super-resolution and colorization on lidar-generated images



(a) Instance segmentation on lidar near-infrared (NIR) images



(b) Instance segmentation on lidar reflectivity image

Fig. 4: Instance segmentation results for different lidar image types. Each image type (subfigure 4a or 4b) shows: original (top-left), result on original (top-right), after CRAN [26] super-resolution (bottom-left), and after super-resolution and Deoldify [6] colorization (bottom-right).

- [25] Y. Tai, J. Yang, and X. Liu. Image super-resolution via deep recursive residual network. In *Proc. of the IEEE Conf. on Computer Vision and Pattern Recognition*, 2017.
- [26] N. Ahn, B. Kang, and K.-A. Sohn. Fast, accurate, and lightweight super-resolution with cascading residual network. *arXiv preprint arXiv:1803.08664*, 2018.
- [27] J. Liang, J. Cao, G. Sun, K. Zhang, L. Van Gool, and R. Timofte. Swinir: Image restoration using swin transformer. *arXiv preprint arXiv:2108.10257*, 2021.
- [28] K. Zhang, Y. Li, J. Liang, J. Cao, Y. Zhang, H. Tang, D.-P. Fan, R. Timofte, and L. V. Gool. Practical blind image denoising via swin-conv-unet and data synthesis. *Machine Intelligence Research*, 20(6), 2023.
- [29] X. Wang, K. Yu, S. Wu, J. Gu, Y. Liu, C. Dong, Y. Qiao, and C. C. Loy. Esgan: Enhanced super-resolution generative adversarial networks. In *The European Conf. on Computer Vision Workshops (ECCVW)*, September 2018.
- [30] J. Yamanaka, S. Kuwashima, and T. Kurita. Fast and accurate image super resolution by deep cnn with skip connection and network in network, 2020.
- [31] Z. Chen, Y. Zhang, J. Gu, Y. Zhang, L. Kong, and X. Yuan. Cross aggregation transformer for image restoration. In *NeurIPS*, 2022.
- [32] J. Johnson, A. Alahi, and L. Fei-Fei. Perceptual losses for real-time style transfer and super-resolution. In *Computer Vision—ECCV: 14th European Conference, Proceedings, Part II 14*. Springer, 2016.
- [33] T. Rott Shaham, T. Dekel, and T. Michaeli. Singan: Learning a generative model from a single natural image. In *Computer Vision (ICCV), IEEE Int. Conf. on*, 2019.
- [34] K. Zhang, W. Zuo, Y. Chen, D. Meng, and L. Zhang. Beyond a Gaussian denoiser: Residual learning of deep CNN for image denoising. *IEEE Transactions on Image Processing*, 26(7), 2017.
- [35] C. Saharia, J. Ho, W. Chan, T. Salimans, D. J. Fleet, and M. Norouzi. Image super-resolution via iterative refinement. *IEEE Transactions on Pattern Analysis and Machine Intelligence*, 45(4), 2023.
- [36] K. Zhang, Y. Li, W. Zuo, L. Zhang, L. Van Gool, and R. Timofte. Plug-and-play image restoration with deep denoiser prior. *IEEE Transactions on Pattern Analysis and Machine Intelligence*, 44(10):6360–6376, 2021.
- [37] L. Qingqing, Y. Xianjia, J. P. Queralt, and T. Westerlund. Multi-modal lidar dataset for benchmarking general-purpose localization and mapping algorithms. In *IEEE/RSJ Int. Conf. on Intelligent Robots and Systems (IROS)*. IEEE, 2022.